Activation of Small Alkanes in Ga-Exchanged Zeolites: A Quantum Chemical Study of Ethane Dehydrogenation

M. V. Frash*,† and R. A. van Santen

Eindhoven University of Technology, P.O. Box 513, 5600 MB Eindhoven, The Netherlands

Received: September 23, 1999; In Final Form: December 20, 1999

Quantum chemical calculations on the mechanism of ethane dehydrogenation catalyzed by Ga-exchanged zeolites have been undertaken. Two forms of gallium, adsorbed dihydridegallium ion $GaH_2^+Z^-$ and adsorbed gallyl ion $[Ga{=}O]^+Z^-$, were considered. It was found that $GaH_2^+Z^-$ is the likely active catalyst. On the contrary, $[Ga{=}O]^+Z^-$ cannot be a working catalyst in nonoxidative conditions, because regeneration of this form is very difficult. Activation of ethane by $GaH_2^+Z^-$ occurs via an "alkyl" mechanism and the gallium atom acts as an acceptor of the ethyl group. The "carbenium" activation of ethane, with gallium abstracting a hydride ion, is much (ca. 51 kcal/mol) more difficult. The catalytic cycle for the "alkyl" activation consists of three elementary steps: (i) rupture of the ethane C−H bond; (ii) formation of dihydrogen from the Brønsted proton and hydrogen bound to Ga; (iii) formation of ethene from the ethyl group bound to Ga. The best estimates (MP2/6-311++G(2df,p)//B3LYP/6-31G*) for the activation energies of these three steps are 36.9, ca. 0, and 57.9 kcal/mol, respectively.

1. Introduction

Transformation of small alkanes in zeolites modified with gallium is a very interesting issue from both industrial and academic point of view.[1] The main industrial application is the conversion of abundant small alkanes to aromatic hydrocarbons (Cyclar process[2]) that are valuable raw chemicals for further synthesis. The academic interest in this transformation is due to the fact that it involves selective activation of the very stable C−H bonds in small alkanes.

A large number of experimental studies on gallium−zeolite catalytic systems have been performed.[1,3−21] Modification of HZSM-5 with only a few weight percentages of gallium significantly increases both the overall rate of alkane activation and selectivity toward aromatics.[1,4−6,8,9,15] The selectivity as high as 60% can be achieved.[1,7] There is strong evidence that dehydrogenation to alkenes is the first step of alkane activation.[1,15,17] Indeed, under certain experimental conditions dehydrogenation is prevailing and alkene plus molecular hydrogen are the main reaction products accompanied by only a small amount of aromatics.[17] It was suggested that the presence of strong Brønsted acid cites together with gallium ions is essential for aromatization activity.[2,13−15] However, recently, Price et al.[19] reported significant dehydrogenation and aromatization activity exhibited by a Ga-exchanged MFI sample with virtually no strong Brønsted cites.

A number of experimental works have addressed the location and oxidation state of gallium in zeolites and its relation to catalytic activity.[1,9,13−16,18−21] Results of this work indicate that only extraframework but not framework gallium species enhance the ZSM-5 activity toward alkanes. Extraframework gallium is introduced into zeolites either by conventional ion exchange technique or by solid-state ion exchange. In both cases, gallium is initially deposed on the outer surface of the zeolite crystals, since hydrated Ga^{3+} ions are too bulky to enter the elliptical channels of ZSM-5.[22] The extracrystalline Ga_2O_3 species are reduced during pretreatment with hydrogen or in contact with hydrocarbon feed and the resulting Ga^{1+} ions migrate into the zeolite channels by surface diffusion.[13,15] Meitzner et al.[13] found that in the working catalyst gallium is present either in the oxidized form Ga^{3+}, or in reduced form, possibly the hydride species GaH_x, bound to zeolite oxygens. The reduced species are detected at high temperature in a reductive atmosphere; however, upon cooling they are transformed to Ga^{3+} even in the flow of hydrogen.

Several suggestions on the reaction mechanism of alkane conversion in Ga-exchanged zeolites have been made in the literature. One option is that the gallium cations and zeolite framework independently promote distinct elementary reactions. However this suggestion is not in agreement with some experimental results, in particular those of Bandiera and Taarit[17] indicating that dehydrogenation and aromatization of ethane occur on the same active center in Ga_2O_3/HAlMFI, as well as with the aromatization activity of the catalysts with proven absence of a separate Ga-containing phase.[19] Another explanation of the catalytic properties of Ga-exchanged zeolites is given by Iglesia et al.[3,12,13,15] These authors stressed that catalysis in the system is essentially bifunctional. Brønsted acid sites are responsible for the C−H bond activation, which yields surface alkyl and H adatom species, whereas Ga sites promote recombination of surface H adatoms to molecular hydrogen. A different mechanism is proposed by Price et al.[19] for alkane conversion in proton-poor Ga-MFI with virtually no strong Brønsted acid sites. They suggested that the catalytic activity arises from the Lewis acid−base pair action of gallium cations and neighboring zeolite oxygen anions.

It is very difficult to experimentally detect all intermediates and find energy parameters for each elementary step involved in a heterogeneous catalytic process. These missing data can be derived from the results of quantum chemical calculations. A reaction of methane with the $[Ga{=}O]^+$ cations in zeolites was considered by Himei et al.[23] and Broclawik et al.[24] These

† Present address: Dept. of Chemistry, York University, Toronto, Ontario, Canada M3J 1P3.

10.1021/jp993414r CCC: $19.00
Published on Web 02/29/2000

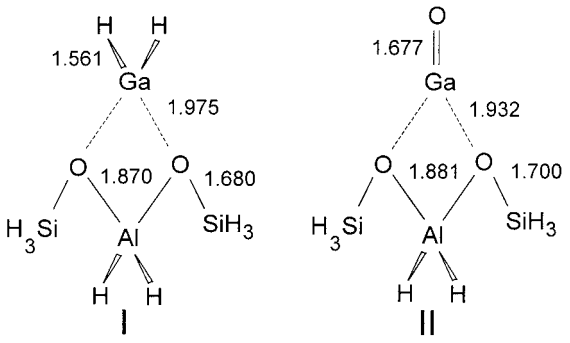

Figure 1. Considered forms of gallium in zeolite: I , adsorbed dihydridegallium ion; II, adsorbed gallyl ion. B3LYP/6-31G* distances in angstroms.

authors computed two reaction products, $[CH_3-Ga-O-H]^+Z^-$ and $[H-Ga-O-CH_3]^+Z^-$ (Z stands for the negative zeolite matrix), as well as the transition state leading to the former product. Two related reactions, activation of methane on alumina and lanthanum oxide, were considered by Capitan et al.[25] These authors calculated products and transition states for the heterolytic dissociation of methane on surface metal−oxygen pairs leading to $CH_3-Me\cdots O-H$ species. However, a full catalytic cycle leading from reactants to products and including regeneration of the active catalyst species was not proposed in either of those works.

The aim of the present quantum chemical study is to propose the full catalytic cycle for dehydrogenation of ethane to ethene in a gallium-exchanged zeolite. As was mentioned above, dehydrogenation can be observed as the predominant reaction at certain experimental conditions, and at the same time is believed to be the first step in the aromatization process. Ethane is the smallest alkane that can yield alkene via monomolecular dehydrogenation. Activation of ethane on pure H-forms of zeolites is particularly difficult; therefore, the role of gallium modifier should be more pronounced for this alkane.

2. Models and Details of Calculations

We consider two distinct models of the Ga species in zeolite: the dihydridegallium ion $GaH_2^+Z^-$ and the gallyl ion $[Ga{=}O]^+Z^-$ (Figure 1). The former ion is a model for GaH_x species coordinated to basic oxygens, according to the Ga K-edge X-ray adsorption measurements of Meitzner et al.[13] The latter ion was suggested as a form of Ga in zeolites by Dooley et al.[26] and considered in the previous quantum chemical studies of Himei et al.[23] and Broclawik et al.[24] on methane activation. The negatively charged zeolite residue Z^- was modeled by the $(H_3SiO)AlH_2(OSiH_3)^-$ cluster. Discussions of the cluster approach and its applications for studies of zeolite catalysts can be found elsewhere.[27−31] Although the cluster approach does not account for some effects such as steric strain and van der Waals interactions, these effects are not expected to qualitatively alter the results. For example, steric effects in the real zeolite might further destabilize the alkoxide,[32] which is involved in the unfavorable reaction route (section 3.2). The van der Waals interactions are expected to be similar for different states, and thus not to significantly affect the computed energy differences.

The Hartree−Fock (HF),[33] second-order Møller−Plesset perturbation theory (MP2)[33] and hybrid nonlocal density functional theory (B3LYP)[34−36] methods were used. Geometries of all the species involved were computed at the B3LYP/6-31G* and HF/6-31G* levels. The 6-31G* basis set is standard for all atoms except Ga. For gallium, we employed the (641) basis set of Binning and Curtiss[37] (recommended for use together with 6-31G). The geometries were fully optimized employing the gradient technique[38] with the "tight" keyword for convergence criteria (force, max. $< 1.5 \times 10^{-5}$; rms, $< 1.0 \times 10^{-5}$; displacement, max. $< 6.0 \times 10^{-5}$; rms, $< 4.0 \times 10^{-5}$ au). The nature of the stationary points obtained was tested by analyzing the (analytically calculated harmonic) vibrational normal modes, at both the B3LYP/6-31G* and HF/6-31G* levels. To ensure that the transition states actually connect the expected reactants and products, each TS geometry was slightly distorted in the forward and reverse direction of the reaction coordinate, and these distorted structures optimized to reach minima. In addition, for the transition states involved in the main reaction route (section 3.1), verification by the intrinsic reaction coordinate (IRC) method[39] was performed and gave the same outcome as the TS distortion method. The calculated total energies and imaginary frequencies of the relevant structures are given in Table 1. The computed weak adsorption complexes between gaseous molecules and the cluster (interaction energies are ca. 2 kcal/mol for ethane and ethene, and less than 0.2 kcal/mol for dihydrogen) are omitted.

TABLE 1: Total Energies of the Investigated Structures (in au) and Imaginary Frequencies (IF) of the Transition States (in cm^{-1})

	HF/6-31G*	IF	B3LYP/6-31G*	IF
		Local Minima		
I	−2896.729250		−2901.010592	
II	−2970.387962		−2975.005754	
IV	−2975.883384		−2980.782650	
VI	−2974.812656		−2979.655037	
IX	−2975.864417		−2980.757326	
XII	−3049.720883		−3054.919662	
XIV	−2971.634948		−2976.272567	
XVI	−3049.702383		−3054.899151	
		Transition States		
III‡	−2975.853151	−1710	−2980.765109	−1102
V‡	−2975.867051	−1298	−2980.778413	−651
VII‡	−2974.697347	−956	−2979.554598	−718
VIII‡	−2975.797639	−538	−2980.703692	−653
X‡	−2975.781400	−951	−2980.699139	−605
XI‡	−3049.560405	−2157	−3054.794282	−1695
XIII‡	−3049.596449	−948	−3054.807520	−745
XV‡	−2971.478046	−1902	−2976.151662	−1501
XVII‡	−3049.502041	−1538	−3054.748234	−776

Reaction enthalpies and activation energies were computed at three levels: MP2(fc)/6-31++G**//HF/6-31G*, B3LYP/6-31++G**//B3LYP/6-31G*, and MP2(fc)/6-31++G**//B3LYP/6-31G*. Corrections for the zero-point energies (ZPE) obtained from the vibrational mode calculations were included (unscaled frequencies were used). Results obtained at the three levels appeared to be reasonably close. Therefore, the MP2(fc)/6-31++G**//B3LYP/6-31G* values will be mainly used in the discussion.

For the main reaction route proposed, higher level MP2(fc)/6-311++(2df,p)//B3LYP/6-31G* calculations were performed. The Gaussian 94 default extension of the 6-311G basis set for second[41] and third[42] row elements was used. DFT calculations with the B3P86[35,43] functional (B3P86/6-31++G**//B3P86/6-31G*) were also performed for the main route. Finally, the effect of the basis set extension from 6-31G* to 6-31++G** at the geometry optimization step was tested in the B3LYP calculations of two structures from the main route. In all cases, only moderate differences between the results from different methods were found.

The calculations of reaction rates (section 3.1) were performed with the MP2(fc)/6-31++G(2df,p)//B3LYP/6-31G* activation barriers. The zero-point and thermal corrections to energies, as

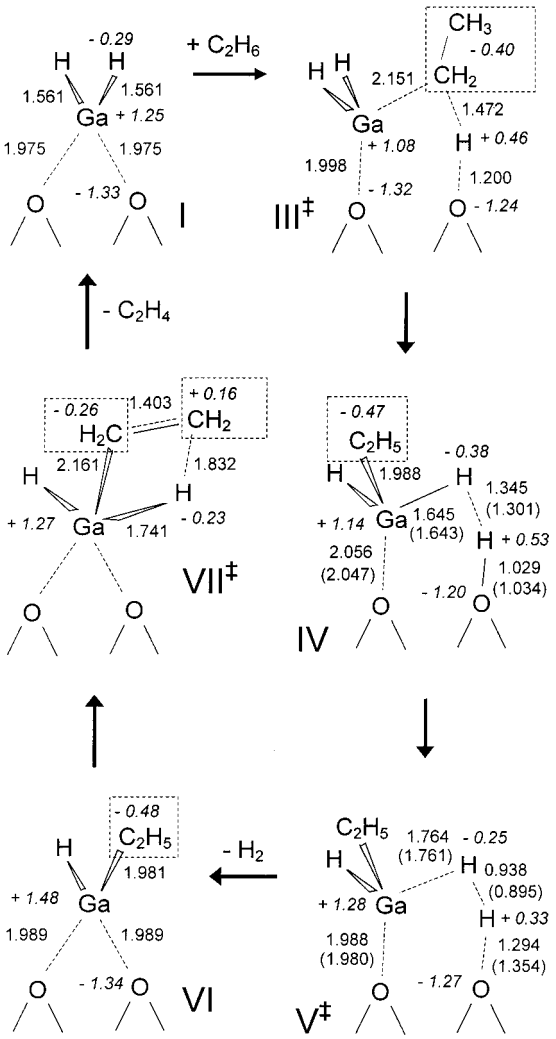

Figure 2. Reaction route for "alkyl" activation of ethane on the adsorbed dihydridegallium ion: (straight figures) B3LYP/6-31G* distances in angstroms; (straight figures in parentheses) B3LYP/6-31++G** distances in angstroms; (italic figures) NPA B3LYP/6-31++G**//B3LYP/6-31G* charges in multiples of the electron charge.

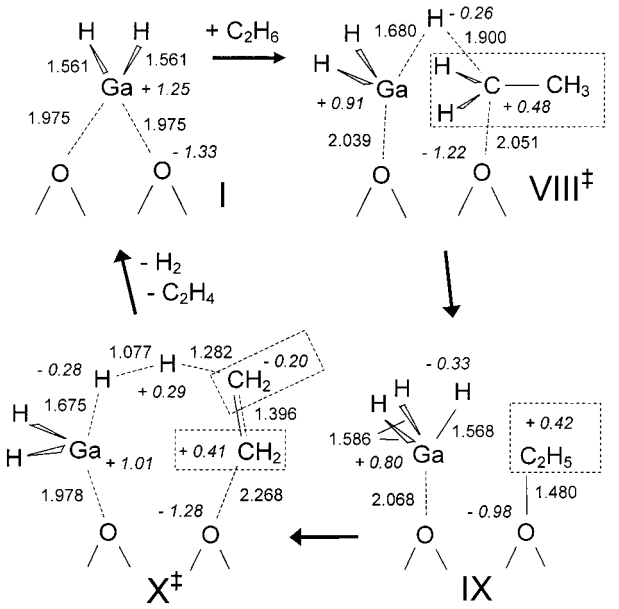

Figure 3. Reaction route for "carbenium" activation of ethane on the adsorbed dihydridegallium ion: (straight figures) B3LYP/6-31G* distances in angstroms; (italic figures) NPA B3LYP/6-31++G**// B3LYP/6-31G* charges in multiples of the electron charge.

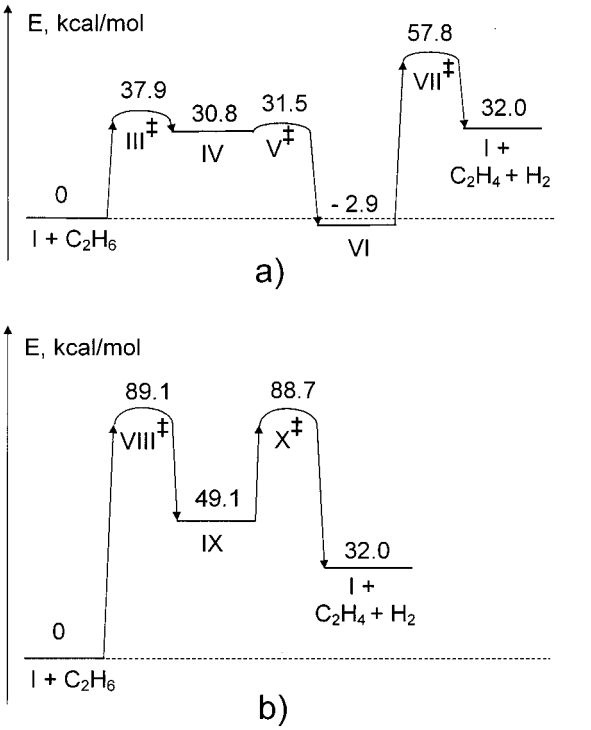

Figure 4. Enthalpies of the intermediates and transition states involved in ethane dehydrogenation on the adsorbed dihydridegallium ion: (a) "alkyl" activation; (b) "carbenium" activation. MP2/6-31++G**// B3LYP/6-31G*.

well as the partition functions (all this quantities require frequencies) were derived from the results of B3LYP/6-31G* calculations.

All the calculations were performed with the Gaussian 94 program.[44] The natural charges[45] were computed using the NBO program[46] incorporated in Gaussian 94.

3. Results

We suggest that two distinct ways of alkane R−H activation on the gallium catalytic site are possible: the "alkyl" activation of a C−H bond ($R^{\delta-}-H^{\delta+}$) and the "carbenium" activation ($R^{\delta+}-H^{\delta-}$). Together with two distinct models of the Ga species in zeolite, $GaH_2^+Z^-$ and $[Ga{=}O]^+Z^-$, this gives four possibilities to be considered: (1) "alkyl" activation on $GaH_2^+Z^-$; (2) "carbenium" activation on $GaH_2^+Z^-$; (3) "alkyl" activation on $[Ga{=}O]^+Z^-$; (4) "carbenium" activation on $[Ga{=}O]^+Z^-$. Below we consider these four reaction routes separately and then compare them.

3.1. Hydride Form of Ga, "Alkyl" Activation of Ethane. The reaction route found for "alkyl" activation of ethane ($C_2H_5^{\delta-}-H^{\delta+}$) on adsorbed dihydridegallium ion $GaH_2^+Z^-$ is shown in Figures 2 and 4a and consists of three elementary steps. These steps can be rationalized in the usual terms of Lewis and Brønsted acid−base interactions.

First Step—Consumption of C_2H_6. The initial structure I contains a Lewis acid, positive Ga atom (charge +1.25 e), and a Lewis base, negative zeolite oxygen (−1.33 e). Together they represent an acid−base pair able to polarize and break a C−H bond of ethane. In the transition state III‡, charges on the leaving hydrogen and the remaining C_2H_5 fragment of ethane are +0.46 and −0.40 e, respectively. The gallium atom then forms a bond with the negative alkyl fragment $C_2H_5^{\delta-}$, while the remaining

TABLE 2: "Alkyl" Activation of Ethane on Adsorbed Dihydridegallium Ion $GaH_2^+Z^-$[a]

	A	B	C	D	E	F
			Enthalpies			
$I + C_2H_6 \rightleftharpoons IV$	+32.8	+30.4		+27.0	+30.8	+30.8
$IV \rightleftharpoons VI + H_2$	−36.0	−27.0		−24.6	−33.7	−29.6
$VI \rightleftharpoons I + C_2H_4$	+35.2	+27.5		+32.8	+34.9	+29.9
$C_2H_6 \rightleftharpoons C_2H_4 + H_2$	+32.0	+30.9		+35.2	+32.0	+31.2
			Activation Energies			
$I + C_2H_6 \rightleftharpoons III^‡$	38.0	41.6		36.1	37.9	36.9
$IV \rightleftharpoons V^‡$	(−1.2)	1.8	2.8	2.1	0.7	(−0.1)
$VI \rightleftharpoons VII^‡$	61.8	57.8		56.1	60.7	57.9

[a] Reaction enthalpies and activation energies (in kcal/mol). A = MP2(fc)/6-31++G**//HF/6-31G*; B = B3LYP/6-31++G**//B3LYP/6-31G*; C = B3LYP/6-31++G**//B3LYP/6-31++G**; D = B3P86/6-31++G**//B3P86/6-31G*; E = MP2(fc)/6-31++G**//B3LYP/6-31G*; F = MP2(fc)/6-311++G(2df,p)//B3LYP/6-31G*.

proton of alkane is "picked up" by the zeolite oxygen. After that, a rotation around the Ga−O axis results in the formation of structure IV, with a strong hydrogen bond. (It is interesting that cleavage of the ethane C−H bond and rotation around the Ga−O bond occur within one step. We could not locate a "prerotational" local minimum rotamer of structure IV.) The first step is endoergic (Table 2), however both the reaction enthalpy (30.8 kcal/mol at the MP2(fc)/6-31++G**//B3LYP/6-31G* level) and activation energy (37.9 kcal/mol) are not prohibitively high.

Second Step—Formation of H_2. Structure IV obtained at the first step contains a strong Brønsted acid (bridge OH group) in the vicinity of the "hydride" hydrogen atoms bound to Ga. One of these "hydride" hydrogens (charge −0.38 e) is located at a short distance (1.345 Å) from the Brønsted proton (charge +0.53 e). This allows one to expect that the H_2 molecule can easily split off from the structure IV. Indeed, a very low activation barrier (0.7 kcal/mol) is found for the exoergic (33.7 kcal/mol) second step.

The overall result of the above considered steps 1 and 2 is the substitution of a hydrogen atom in dihydridegallium ion by the ethyl group of ethane and release of dihydrogen

$$GaH_2^+Z^- + C_2H_6 \rightleftharpoons [Ga(H)(C_2H_5)]^+Z^- + H_2 \quad (1a)$$

It is therefore conceivable that the reaction 1a can proceed in one step rather than in two steps. We computed a transition state for the one-step reaction 1a and found an activation barrier of 52.2 kcal/mol (MP2/6-31++G**//B3LYP/6-31G*). This barrier is about 14 kcal/mol higher than that for the two-step reaction sequence. Thus, the sequence of steps 1 and 2 will occur easier than reaction 1a. Note that the zeolite oxygen atom does not participate in reaction 1a but participates in the steps 1 and 2, first picking up the proton and then releasing it to produce dihydrogen. Thus, the zeolite oxygen "catalyzes" the substitution of the hydrogen atom in GaH_2^+ by the ethyl group.

Third Step—Formation of C_2H_4. Structure VI obtained at the second step contains the ethyl group (C_2H_5) bound to the positively charged (+1.48 e) gallium atom. The latter can abstract a hydride anion from the β-position of the ethyl group. Indeed, in the transition state $VII^‡$, the shifting hydrogen bears a negative charge (−0.23 e), while the remaining β-methylene group is positively charged (+0.16 e). After this step, the ethene molecule is formed and the initial dihydridegallium ion I is regenerated. The third step is endoergic (34.9 kcal/mol) and has an activation barrier of 60.7 kcal/mol.

Sensitivity of the Results to the Level of Calculations. Comparison of the considered above route 1 with other routes (see below) indicates that route 1 is the main one for ethane dehydrogenation. Therefore, we performed higher level (MP2-(fc)/6-311++G(2df,p)//B3LYP/6-31G*) calculations of reaction enthalpies and activation energies of the elementary steps involved. The results obtained are given in Table 2. These results are not far (typically within 4 kcal/mol) from the results obtained at other levels, including MP2 with a smaller basis set, B3LYP, and B3P86. Thus, sensitivity of the results to the level of calculations within the selected set of levels is moderate. The best estimates obtained for the activation energies of the three elementary steps involved in the main reaction route are 36.9, ca. 0, and 57.9 kcal/mol, respectively.

TABLE 3: Rate Constants k_r for the Main Reaction Route and Reaction Rates per Mole of Ga (Partial Pressure of Ethane is 13.3 kPa[17])

reaction	$E^‡$ kcal/mol	A	k_r	rate per mol of Ga, mol s^{-1}
		500 K		
step 1	37.9	9.65×10^3	2.74×10^{-13} [a]	8.77×10^{-13}
step 2	(0)	1.14×10^{12}	1.14×10^{12} [b]	1.14×10^{12}
step 3	57.2	2.07×10^{11}	2.00×10^{-14} [b]	2.00×10^{-14}
		700 K		
step 1	39.0	2.23×10^4	1.54×10^{-8} [a]	3.52×10^{-8}
step 2	(0)	1.23×10^{12}	1.23×10^{12} [b]	1.23×10^{12}
step 3	57.2	2.47×10^{11}	2.59×10^{-7} [b]	2.59×10^{-7}
		900 K		
step 1	40.0	4.36×10^4	8.15×10^{-6} [a]	1.45×10^{-5}
step 2	(0)	1.37×10^{12}	1.37×10^{12} [b]	1.37×10^{12}
step 3	57.2	3.02×10^{11}	3.83×10^{-3} [b]	3.83×10^{-3}

[a] In m^3 mol^{-1} s^{-1}. [b] In s^{-1}.

As was suggested by a reviewer of this paper, we also tested the effect of the geometry optimization with the 6-31++G** instead of 6-31G* basis set. The activation energy of the second step of the main route was chosen for this test. Our calculations based on the geometry optimization with the 6-31G* basis set predicted a very low activation barrier for this step (from 0 to 2.1 kcal/mol; see Table 2). However, there are experimental indications that this step is difficult.[12] We reoptimized geometries of structures IV and $V^‡$ (Figure 2) at the B3LYP/6-31++G** level. This led to some changes in the computed geometric parameters (up to 0.04−0.06 Å for the O−H bond being broken and H−H bond being formed). However, the activation energy computed at B3LYP/6-31++G**//B3LYP/6-31++G** differs by 1 kcal/mol only from that at B3LYP/6-31++G**//B3LYP/6-31G*. Therefore, use in the most of calculations of the more compact 6-31G* basis set instead of 6-31++G** is not expected to introduce a significant error in the computed enthalpies and activation energies.

Heats of the dehydrogenation reaction $C_2H_6 \rightleftharpoons C_2H_4 + H_2$ obtained from the MP2 and B3LYP final energies are within 30.9−32.0 kcal/mol (Table 2). This is in a good agreement with the experimental value of 30.9 kcal/mol derived from the heats of formation at 0 K (C_2H_6, −16.4; C_2H_4, 14.5; H_2, 0)[47] The B3P86/6-31++G**//B3P86/6-31G* value (35.2 kcal/mol) differs more from experiment.

Calculation of the Reaction Rates and Comparison with the Experimental Data. The rate constants for all three steps of the main reaction route were computed based on the transition state theory:[48]

$$k_r = A \exp(-E^‡/(RT))$$

The computed activation energies $E^‡$, pre-exponential factors A, and rate constants k_r at 500, 700, and 900 K are given in Table 3. The calculation procedure is described elsewhere.[49]

TABLE 4: Reaction Enthalpies and Activation Energies (in kcal/mol) for "Carbenium" Activation of Ethane on Adsorbed Dihydridegallium Ion $GaH_2^+Z^-$

	MP2(fc)/ 6-31++G**// HF/6-31G*	B3LYP/ 6-31++G**// B3LYP/6-31G*	MP2(fc)/ 6-31++G**// B3LYP/6-31G*
	Enthalpies		
$I + C_2H_6 \rightleftharpoons IX$	+ 49.7	+ 50.6	+ 49.1
$IX \rightleftharpoons I + C_2H_4 + H_2$	−17.6	−19.8	−17.1
	Activation Energies		
$I + C_2H_6 \rightleftharpoons VIII^‡$	90.0	81.1	89.1
$IX \rightleftharpoons X^‡$	40.5	29.4	39.6

To find the rate-determining step, one needs to compare the relative rates of the three consecutive elementary reactions. The rate constant of the bimolecular first step and those of the monomolecular second and third steps are measured in different units ($m^3\ mol^{-1}\ s^{-1}$ vs s^{-1}) and cannot be directly compared. Therefore, we computed the reaction rate per mole of Ga for all three steps. This rate is numerically equal to the rate constant for the monomolecular steps and to the product of the rate constant and ethane concentration in mol m^{-3} for the bimolecular first step (Table 3). The ethane concentration at the pressure of 13.3 kPa (experimental conditions in the work of Bandiera and Taarit[17]) was used.

Reaction rates given in Table 3 indicate that the third step is the slowest at 500 K, due to its high activation energy. However, the first step appears to be the slowest at higher temperatures of 700 and 900 K, due to its low pre-exponential factor. The low pre-exponential factor for the first step is a result of a large entropy loss in the surface activated complex with respect to the gas-phase ethane molecule.

We found only one experimental work that reported the activation energy for ethane dehydrogenation in Ga-exchanged zeolites.[17] The value of 163 kJ/mol (39.0 kcal/mol) was obtained at 720−820 K, ethane partial pressure of 13.3 kPa, high flow rate, and low conversion. According to the data of Table 3, the first step is the rate-determining one at this temperature and pressure. Indeed, the calculated activation energy of 39−40 kcal/mol (MP2(fc)/6-311++G(2df,p)//B3LYP/6-31G* plus zero-point and thermal corrections) for the first step is very close to the reported experimental value.

3.2. Hydride Form of Ga, "Carbenium" Activation of Ethane. *First Step— Consumption of C_2H_6.* In principle, the $Ga^{\delta+}-O^{\delta-}$ Lewis pair can cause $C_2H_5{}^{\delta+}-H^{\delta-}$ polarization of the ethane molecule, instead of the above considered $C_2H_5{}^{\delta-}-H^{\delta+}$ polarization. Indeed, charges on the ethyl group (+0.48 e) and the shifting hydrogen atom (−0.26 e) in the transition state VIII‡ (Figure 3) are opposite to those in the TS III‡ for "alkyl" activation. Then the gallium atom forms a bond with the negative hydrogen atom, while the remaining alkyl fragment $C_2H_5{}^{\delta+}$ binds to the zeolite oxygen. This step is endoergic (49.1 kcal/mol) and has a very high activation barrier (89.1 kcal/mol at the MP2/6-31++G**//B3LYP/6-31G* level, Table 4). This activation barrier is much (ca. 51 kcal/mol) higher than that for the above considered "alkyl" activation.

Second Step—Formation of C_2H_4 and H_2. At the second step of this route, the $C^{\delta+}-O^{\delta-}$ bond of structure IX undergoes elongation (from 1.480 Å in IX to 2.268 Å in the transition structure X‡). Simultaneously, the positive β-hydrogen (charge +0.29 e) of the ethyl group approaches the "hydride" hydrogen (charge −0.28 e) bound to Ga. The H−H distance in X‡ is 1.077 Å, instead of 5.173 Å in IX. The second step is exoergic (17.1 kcal/mol) and results in the formation of dihydrogen and ethene and regeneration of the initial dihydridegallium ion I. The activation barrier for this step is 39.6 kcal/mol.

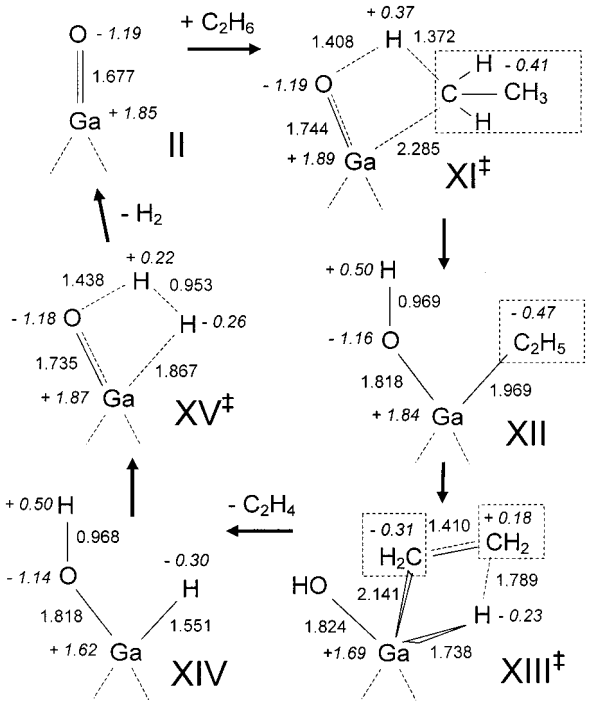

Figure 5. Reaction route for "alkyl" activation of ethane on the adsorbed gallyl ion: (straight figures) B3LYP/6-31G* distances in angstroms; (italic figures) NPA B3LYP/6-31++G**//B3LYP/6-31G* charges in multiples of the electron charge.

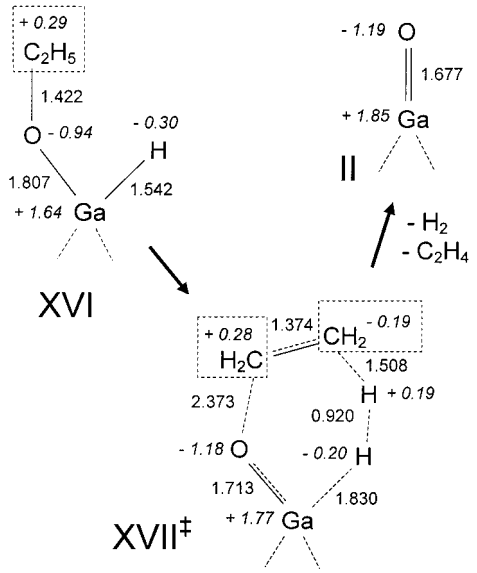

Figure 6. Regeneration of the adsorbed gallyl ion after "carbenium" activation of ethane: (straight figures) B3LYP/6-31G* distances in angstroms; (italic figures) NPA B3LYP/6-31++G**//B3LYP/6-31G* charges in multiples of the electron charge.

Because of the very high barrier for the first step, the "carbenium" activation of ethane on adsorbed dihydridegallium ion $GaH_2^+Z^-$ is unlikely to occur.

3.3. Oxidized Form of Ga, "Alkyl" Activation of Ethane. *First Step—Consumption of C_2H_6.* The gallium and oxygen atoms of the gallyl ion $[Ga{=}O]^+$ represent a Lewis acid−base pair able to polarize and break the ethane $C^{\delta-}-H^{\delta+}$ bond. Similar to route 1, the gallium atom can form a bond with the negative alkyl fragment $C_2H_5{}^{-\delta}$, while the remaining proton of alkane binds to oxygen (Figures 5 and 7a). Charges on the ethyl group (−0.41 e) and the shifting hydrogen atom (+0.37 e) in the transition state XI‡ (Figure 3) are similar to those in the TS

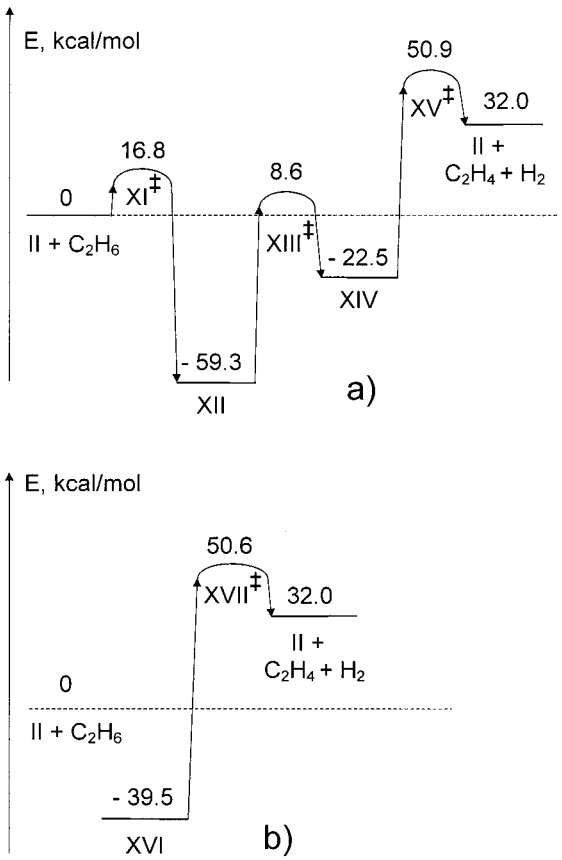

Figure 7. Enthalpies of the intermediates and transition states involved in (a) "alkyl" activation of ethane on the adsorbed gallyl ion and (b) regeneration of the adsorbed gallyl ion after "carbenium" activation. MP2/6-31++G**//B3LYP/6-31G*.

TABLE 5: Reaction Enthalpies and Activation Energies (in kcal/mol) for "Alkyl" Activation of Ethane on Adsorbed Gallyl Ion $[Ga{=}O]^+Z^-$

	MP2(fc)/ 6-31++G**// HF/6-31G*	B3LYP/ 6-31++G**// B3LYP/6-31G*	MP2(fc)/ 6-31++G**// B3LYP/6-31G*
	Enthalpies		
$II + C_2H_6 \Rightarrow XII$	−59.3	−56.7	−59.3
$XII \Rightarrow XIV + C_2H_4$	+37.0	+29.7	+36.8
$XIV \Rightarrow II + H_2$	+54.4	+57.7	+54.5
	Activation Energies		
$II + C_2H_6 \Rightarrow XI^‡$	16.6	19.8	16.8
$XII \Rightarrow XIII^‡$	69.2	65.5	67.9
$XIV \Rightarrow XV^‡$	74.2	74.0	73.4

III‡ of route 1. This step is highly exoergic (59.3 kcal/mol mol at the MP2/6-31++G**//B3LYP/6-31G* level, Table 5) and has a rather low activation energy (16.8 kcal/mol). This activation energy is much lower than that for the ethane activation on the dihydridegallium ion (37.9 kcal/mol) considered in the section 3.1. Thus, the adsorbed gallyl ions $[Ga{=}O]^+Z^-$ should easily react with ethane. However, to be the working catalyst, these ions need to be regenerated.

Second Step—Formation of C_2H_4. Structure XII obtained at the first step contains a negative ethyl group bound to the gallium atom. Stretching of the carbon−gallium bond enhances its $C^{\delta-}-Ga^{\delta+}$ polarization and therefore increases the Lewis acid strength of the Ga cation. This cation abstracts a hydride anion from the β-position of the ethyl group. Then, the ethene molecule and the adsorbed hydroxyhydridegallium cation XIV are formed. This step is endoergic (36.8 kcal/mol) and has an activation barrier of 67.9 kcal/mol.

TABLE 6: Reaction Enthalpy and Activation Energy (in kcal/mol) for Regeneration of the Adsorbed Gallyl Ion $[Ga{=}O]^+Z^-$ After "Carbenium" Activation of Ethane

	MP2(fc)/ 6-31++G**// HF/6-31G*	B3LYP/ 6-31++G**// B3LYP/6-31G*	MP2(fc)/ 6-31++G**// B3LYP/6-31G*
	Enthalpy		
$XVI \Rightarrow II + C_2H_4 + H_2$	+ 71.3	+ 70.7	+ 71.5
	Activation Energy		
$XVI \Rightarrow XVII^‡$	90.7	85.8	90.1

It is interesting that structure XII resembles structure VI from route 1 and transition state XIII‡ resembles TS VII‡ from route 1. The difference consists of the presence of the (Ga)−OH group in XII and XIII‡, instead of (Ga)−H in VI and VII‡. Comparison of the data given in Tables 2 and 5 indicates that substitution of (Ga)−H for (Ga)−OH increases the activation energy for this step by about 7 kcal/mol.

Third Step—Formation of H_2. Structure XIV obtained at the second step can be transformed back to the initial adsorbed gallyl ion, if the hydrogen atoms of the (Ga)−H and (Ga)−OH groups form a dihydrogen molecule and split off. However, this reaction is calculated to be highly endoergic (54.5 kcal/mol) and to have a high activation energy (73.4 kcal/mol).

Most importantly, the sum of reaction enthalpies for the second and third step is positive and very high (91.3 kcal/mol). In other words, structure XII (adsorbed ethylhydroxygallium cation) is ca. 91 kcal/mol lower in energy than the initial structure II (adsorbed gallyl cation). This means that the thermodynamical equilibrium between the two structures will be almost fully shifted toward XII, and formation of II practically will not take place.

These results indicate that the adsorbed gallyl ions $[Ga{=}O]^+Z^-$ cannot be the working catalyst in the feed containing only hydrocarbons and hydrogen. If the $[Ga{=}O]^+Z^-$ species are present in the initial zeolite, they will rapidly react with hydrocarbons and the Ga=O bond will be transformed to a single bond. However, regeneration of the $[Ga{=}O]^+Z^-$ species is thermodynamically prohibited. Instead of this, it is likely that there will be formed other active forms of gallium, possibly the $GaH_2^+Z^-$ species considered above (sections 3.1 and 3.2). This conclusion is not necessarily applicable to the oxidative dehydrogenation, because in that case reduction of the oxidants such as O_2 or NO_x might provide extra energy required for regeneration of the $[Ga{=}O]^+Z^-$ species.

3.4. Oxidized Form of Ga, "Carbenium" Activation of Ethane. We have shown above that regeneration of the $[Ga{=}O]^+Z^-$ species after the "alkyl" activation of ethane is very difficult. Now we consider regeneration of these species after the "carbenium" activation. A "carbenium" ($C_2H_5^{\delta+}-H^{\delta-}$) cleavage of the ethane bond on the $Ga^{\delta+}{=}O^{\delta-}$ pair would lead to structure XVI (Figure 6), which is lower in energy than the reactants by 39.5 kcal/mol mol (MP2/6-31++G**//B3LYP/6-31G*). Structure XVI could be transformed back to $[Ga{=}O]^+Z^-$, if the C−O bond breaks and one β-hydrogen of the ethyl group binds to the hydrogen of the Ga−H group (Figures 6 and 7b). This reaction is highly endoergic (71.5 kcal/mol) and has a very high activation barrier (90.1 kcal/mol) (Table 6). This indicates that regeneration of the initial adsorbed gallyl ion $[Ga{=}O]^+Z^-$ from the adsorbed ethoxyhydridegallium ion XVI is practically impossible. Therefore, the $[Ga{=}O]^+$ species cannot be the working catalysts in the cycle starting from the "carbenium" activation of ethane.

Thus, the results of calculations indicate that the "alkyl" activation on the $GaH_2^+Z^-$ species represents the main reaction

route for ethane dehydrogenation in Ga-exchanged zeolites. The "carbenium" activation on $GaH_2^+Z^-$ is ruled out because of the very high activation energy for the first step. The $[Ga{=}O]^+Z^-$ species are thermodynamically unfavorable, and their regeneration under the (nonoxidative) reaction conditions is very difficult. Therefore, these species are ruled out as the working catalyst either for "alkyl" or "carbenium" activation of ethane.

4. Discussion

The results of our calculations suggest that the "alkyl" route discussed in section 3.1 is the likely catalytic cycle for ethane dehydrogenation in Ga-exchanged zeolites. Now we compare this catalytic cycle to the experimental data and mechanistic proposals derived from them.

According to our results, the $GaH_x^{\delta+}$ species are the working catalytic form. This prediction is in full agreement with the K-edge X-ray measurements of Meitzner et al.[13]

Participation of the zeolite oxygen together with the gallium atom in the alkane activation step follows from the results of calculations. This is in agreement with the mechanism proposed by Price et al.[19]

However, the direction of the alkane C−H bond polarization during activation predicted from the results of calculations is different from that assumed in the literature. Indeed, a number of authors[1,12] suggested that gallium acts as a hydride ion acceptor and the bond polarization is $C^{\delta+}-H^{\delta-}$. In contrast, our calculations indicate that gallium preferentially acts as an alkyl anion acceptor and therefore the ethane bond polarization is $C^{\delta-}-H^{\delta+}$. Note that our result is in line with the higher electronegativity of carbon with respect to hydrogen (2.5 vs 2.1 in the Pauling's scale),[50] as well as with the low stability of the primary ethyl carbenium ion (that should be formed in the case of hydride abstraction).

This conclusion on the direction of C−H bond polarization cannot be automatically transferred to alkanes larger than ethane, since upon hydride abstraction they form more stable secondary and tertiary carbenium ions instead of the primary ethyl cation. However it should be noted that the calculated difference in activation energies between carbenium and alkyl activation (ca. 51 kcal/mol) is larger than the stabilization energy of free secondary and tertiary carbenium ions (19 and 38 kcal/mol, respectively[51]) with respect to the ethyl cation. The difference in stability of primary, secondary, and tertiary carbocations in zeolites is even smaller than in the gas phase,[52−54] since adsorbed carbocations are not free but interact with the zeolite oxygens,[55] and this interaction is stronger for the otherwise less stable ions. Therefore, we can suggest that even for larger alkanes $C^{\delta-}-H^{\delta+}$ polarization and alkyl abstraction by Ga will be preferred over $C^{\delta+}-H^{\delta-}$ polarization and hydride abstraction.

According to Iglesia et al.,[3,12,13,15] gallium in a zeolite works as a "porthole" for recombination of surface hydrogen atoms to dihydrogen molecules. This elementary step is indeed present in our calculated reaction route (step 2 of route 1). However, the computed activation energy for this step is very small (less than 2 kcal/mol), in contrast to the kinetic data[12] indicating that this step is difficult. The reason for this discrepancy is unknown. It might be that a higher activation energy is required for hydrogen recombination when the Ga−H and O−H groups are spatially more separated.

The results of calculations indicate that the reaction $[Ga]-C_2H_5 \rightleftharpoons C_2H_4 + [Ga]-H$ is involved in ethane dehydrogenation. It is interesting that such a reaction was not proposed (to our knowledge) in the publications devoted to Ga-containing zeolites. However, we found that a similar type of reaction was proposed to explain the activity of a $Zr-H/SiO_2$ catalyst for C−H and C−C bond cleavage in alkanes.[56] The authors[56] prepared a silica-supported zirconium hydride catalyst that converts alkanes larger than ethane (in the presence of hydrogen) into the mixture of methane and ethane at room temperature. The proposed reaction mechanism[56] is based on the heterolytic cleavage of the Zr−C bond followed by the β-hydrogen or β-methyl transfer to zirconium.

Thus, the reaction mechanism for ethane dehydrogenation in Ga-exchanged zeolites found in our calculations is in agreement with most experimental observations and mechanistic proposals based on them.

Finally, we compare the computational results for dehydrogenation of ethane in Ga-exchanged zeolites and in the H-forms of zeolites. In the latter case, the reaction involves a "carbenium" ($C^{\delta+}-H^{\delta-}$) activation of the ethane C−H bond, which requires a high activation energy (71−84 kcal/mol, dependent on the acid site model and computational method).[57,58] As shown in the present work, the "alkyl" activation route for ethane in the presence of Ga involves much lower activation barriers (36.9 kcal/mol for the C−H bond rupture and 57.9 kcal/mol for the release of ethene from the catalytic site). Thus, the catalytic effect of gallium is due to the replacement of the high-barrier "carbenium" activation of ethane by the lower barrier "alkyl" activation.

5. Conclusion

Quantum chemical calculations on the mechanism of ethane dehydrogenation catalyzed by Ga-exchanged zeolites were performed, revealing the following.

(1) Gallium hydride species ($GaH_x^{\delta+}$) bound to the zeolite oxygen are likely the active catalytic form of gallium. In contrast, the gallyl ion $[Ga{=}O]^+$ cannot be a working catalyst in non-oxidative conditions. The gallyl ion will readily react with ethane but will not be regenerated.

(2) Activation of ethane occurs via "alkyl" polarization and rupture of a C−H bond ($C_2H_5^{\delta-}-H^{\delta+}$). The Ga atom acts as an ethyl group acceptor during ethane activation, rather than a hydride ion acceptor. "Carbenium" activation ($C_2H_5^{\delta+}-H^{\delta-}$) is much more difficult because of the higher electronegativity of carbon with respect to hydrogen, and the low stability of the primary ethyl cation.

(3) The catalytic cycle for ethane transformation to ethene and dihydrogen consists of three elementary steps: (i) rupture of the ethane C−H bond; (ii) formation of dihydrogen from the Brønsted proton and the hydrogen bound to Ga; (iii) formation of ethene from the ethyl group bound to Ga.

(4) A number of calculation levels (MP2/6-31++G**//HF/6-31G*, B3LYP/6-31++G** //B3LYP/6-31G*, MP2/6-31++G**//B3LYP/6-31G*, and MP2/6-311++G(2df,p)//B3LYP/6-31G*) were tested, and the results were found to be similar. The best estimates (the latter level) for the activation energies of the three elementary steps involved in the main reaction route are 36.9, ca. 0, and 57.9 kcal/mol, respectively.

Supporting Information Available: Cartezian atomic coordinates of the structures I−XVII‡, computed at the B3LYP/6-31G* level. This material is available free of charge via the Internet at http://pubs.acs.org.

References and Notes

(1) Ono, Y. *Catal. Rev.—Sci. Eng.* **1992**, *34*, 179.

(2) Mowry, J. R.; Anderson, R. F.; Johnson, J. A. *Oil Gas J.* **1985**, *83*, 128.

(3) Iglesia, E.; Barton, D. G.; Biscardi, J. A.; Gines, M. J. L.; Soled, S. L. *Catal. Today* **1997**, *38*, 339.
(4) Sirokman, G.; Sendola, Y.; Ono, Y. *Zeolites* **1980**, *6*, 299.
(5) Mole, T.; Anderson, J. R.; Greer, G. *Appl. Catal.* **1985**, *17*, 141.
(6) Bragin, O. V.; Vasina, T. V.; Isaev, S. A.; Kudryavtseva, G. A.; Sytnyk, V. P.; Preobrazhensky, A. V. *Bull. Acad. Sci. USSR, Div. Chem. Sci.* **1988**, *37*, 24.
(7) Minachev, Kh. M.; Bragin, O. V.; Vasina, T. V.; Dergachev, A. A.; Shpiro, E. S.; Sytnyk, V. P.; Bondarenko, T. N.; Tkachenko, O. P.; Preobrazhenskii, A. V. *Dokl. Akad. Nauk SSSR* **1988**, *304*, 1391.
(8) Gnep., N. S.; Dojemet, J. Y.; Seco, A. M.; Ribeiro, F. R.; Guisnet, M. *Appl. Catal.* **1988**, *43*, 155.
(9) Yakerson, V. I.; Vasina, T. V.; Lafer, L. I.; Sytnyk, V. P.; Dykh, G. L.; Mokhov, A. V.; Bragin, O. V.; Minachev, Kh. M. *Catal. Lett.* **1989**, *3*, 339.
(10) Ono, Y.; Nakatini, H.; Kitagawa, H.; Suzuki, E. *Stud. Surf. Sci. Catal.* **1989**, *44*, 279.
(11) Ono, Y.; Kanae, K. *J. Chem. Soc., Faraday Trans.* **1991**, *87*, 669.
(12) Iglesia, E.; Baumgartner, J. E.; Price, G. L. *J. Catal.* **1992**, *134*, 549.
(13) Meitzner, G. D.; Iglesia, E.; Baumgartner, J. E.; Huang, E. S. *J. Catal.* **1993**, *140*, 209.
(14) Price, G. L.; Kanazirev, V. I.; Dooley, K. M. *Zeolites* **1995** *15*, 725.
(15) Biscardi, J. A.; Iglesia, E. *Catal. Today* **1996**, *31*, 207.
(16) Sulikowski, B.; Olejniczak, Z.; Corberan, V. C. *J. Phys. Chem.* **1996**, *100*, 10323.
(17) Bandiera, J.; Taarit, Y. B. *Appl. Catal. A* **1997**, *152*, 43.
(18) Chao, K. J.; Sheu, S. P.; Lin, L.-H.; Genet, M. J.; Feng, M. H. *Zeolites* **1997**, *18*, 18.
(19) Price, G. L.; Kanazirev, V.; Dooley, K. M.; Hart, V. I. *J. Catal.* **1998**, *173*, 17.
(20) Takeguchi, T.; Kim, J.-B.; Kang, M.; Inui, T.; Cheuh, W.-T.; Haller, G. L. *J. Catal.* **1998**, *175*, 1.
(21) Brabec, L.; Jeschke, M.; Klik, R.; Novakova, J.; Kubelkova, L.; Freude, D.; Bosacek, V.; Meusinger, J. *Appl. Catal. A* **1998**, *167*, 309.
(22) Kaliaguine, S.; Lemay, G.; Adnot, A.; Burelle, S.; Audet, R.; Jean, G.; Sawicki, J. A. *Zeolites* **1990**, *10*, 559.
(23) Himei, H.; Yamadaya, M.; Kubo, M.; Vetrivel, R.; Broclawik, E.; Miyamoto, A. *J. Phys. Chem.* **1995**, *99*, 12461.
(24) Broclawik, E.; Himei, H.; Yamadaya, M.; Kubo, M.; Miyamoto, A.; Vetrivel, R. *J. Chem. Phys.* **1995**, *103*, 2102.
(25) Capitan, M. J.; Odriozola, J. A.; Marquez, A.; Fernandez Sanz, J. *J. Catal.* **1995**, *156*, 273.
(26) Dooley, K. M.; Chang, C.; Price, G. L. *Appl. Catal. A* **1992**, *84*, 17.
(27) Sauer, J.; Ugliengo, P.; Garrone, E.; Saunders, V. R. *Chem. Rev.* **1994**, *94*, 2095.
(28) Kramer, G. J.; Van Santen, R. A. *Chem. Rev.* **1995**, *95*, 637.
(29) Blaszkowski, S. R.; Van Santen, R. A. *Top. Catal.* **1997**, *4*, 145.
(30) Van Santen, R. A. *Catal. Today* **1997**, *38*, 377.
(31) Nicholas, J. B. *Top. Catal.* **1997**, *4*, 157.
(32) Sherwood, P.; de Vries, A. H.; Collins, S. J.; Greatbanks, S. P.; Burton, N. A.; Vincent, M. A.; Hillier, I. H. *Faraday Discuss.* **1997**, *106*, 79.
(33) Hehre, W. J.; Radom, L.; Schleyer, P. v R.; Pople, J. A. *Ab Initio Molecular Orbital Theory*; John Wiley and Sons: New York, 1986.
(34) Stephens, P. J.; Devlin, F. J.; Chabalowski, C. F.; Frisch, M. J. *J. Phys. Chem.* **1994**, *98*, 1623.
(35) (a) Becke, A. D. *J. Chem. Phys.* **1993**, *98*, 1372; (b) **1993**, *98*, 5648.
(36) Lee, C.; Yang, W.; Parr, R. G. *Phys. Rev. B* **1988**, *37*, 785.
(37) Binning, R. C.; Curtiss, L. A. *J. Comput. Chem.* **1990**, *11*, 1206.
(38) Schlegel, H. B. *J. Comput. Chem.* **1982**, *3*, 214.
(39) Gonzalez, C.; Schlegel, H. B. *J. Chem. Phys.* **1989**, *90*, 2154.
(40) Gonzalez, C.; Schlegel, H. B. *J. Phys. Chem.* **1990**, *94*, 5523.
(41) McLean, A. D.; Chandler, G. S. *J. Chem. Phys.* **1980**, *72*, 5639.
(42) Curtiss, L. A.; McGrath, M. P.; Blaudeau, J.-P.; Davis, N. E.; Binning, R. C., Jr.; Radom, L. *J. Chem. Phys.* **1995**, *103*, 6104.
(43) Perdew, J. P. *Phys. Rev. B* **1986**, *33*, 8822.
(44) Frisch, M. J.; Trucks, G. W.; Schlegel, H. B.; Gill, P. M. W.; Johnson, B. G.; Robb, M. A.; Cheeseman, J. R.; Keith, T.; Petersson, G. A.; Montgomery, J. A.; Raghavachari, K.; Al-Laham, M. A.; Zakrzewski, V. G.; Ortiz, J. V.; Foresman, J. B.; Cioslowski, J.; Stefanov, B. B.; Nanayakkara, A.; Challacombe, M.; Peng, C. Y.; Ayala, P. Y.; Chen, W.; Wong, M. W.; Andres, J. L.; Replogle, E. S.; Gomperts, R.; Martin, R. L.; Fox, D. J.; Binkley, J. S.; Defrees, D. J.; Baker, J.; Stewart, J. P.; Head-Gordon, M.; Gonzalez, C.; Pople, J. A. *Gaussian 94*, revision B.3; Gaussian, Inc.: Pittsburgh, PA, 1995.
(45) Reed, A. E.; Curtiss, L. A.; Weinhold, F. *Chem. Rev.* **1988**, *88*, 899.
(46) Glendening, E. D.; Reed, A. E.; Carpenter, J. E.; Weinhold, F. *NBO*, version 3.1.
(47) Lias, S. G.; Bartmess, J. E.; Liebman, J. F.; Holmes, J. L.; Levin, R. D.; Mallard, W. G. *J. Phys. Chem. Ref. Data* **1988**, *17* (Suppl. 1), p 40.
(48) Moore, J. W.; Pearson, R. G. *Kinetics and Mechanisms*; John Wiley & Sons: New York, 1981.
(49) Blaszkowski, S. R.; Jansen, A. P. J.; Nascimento, M. A. C.; Van Santen, R. A. *J. Phys. Chem.* **1994**, *98*, 12938.
(50) Phillips, C. S. G.; Williams, R. J. P. *Inorganic Chemistry*; Oxford University Press: Oxford, 1965; p 114.
(51) Lossing, F. P.; Holmes, J. L. *J. Am. Chem. Soc.* **1984**, *106*, 6917.
(52) Rigby, A. M.; Kramer, G. J.; Van Santen, R. A. *J. Catal.* **1997**, *170*, 1.
(53) Kazansky, V. B.; Frash, M. V.; Van Santen, R. A. *Catal. Lett.* **1997**, *48*, 61.
(54) Frash, M. V.; Kazansky, V. B.; Rigby, A. M.; Van Santen, R. A. *J. Phys. Chem. B* **1998**, *102*, 2232.
(55) Kazansky, V. B. *Acc. Chem. Res.* **1991**, *24*, 379.
(56) Corker, J.; Lefebvre, F.; Lecuyer, C.; Dufaud, V.; Quignard, F.; Choplin, A.; Evans, J.; Basset, J.-M. *Science* **1996**, *271*, 966.
(57) Blaszkowski, S. R.; Nascimento, M. A. C.; Van Santen, R. A. *J. Phys. Chem.* **1996**, *100*, 3463.
(58) Kazansky, V. B.; Frash, M. V.; Van Santen, R. A. *Appl. Catal. A* **1996**, *146*, 225.